Implications of climate change on wind erosion of agricultural lands in the Columbia plateau

B.S. Sharratt [a,*], J. Tatarko [b], J.T. Abatzoglou [c], F.A. Fox [b], D. Huggins [a]

[a] USDA-ARS, 215 Johnson Hall, WSU, Pullman, WA 99164, USA
[b] USDA-ARS, 2150 Centre Ave., Ft. Collins, CO 80526, USA
[c] University of Idaho, McClure Hall, Moscow, ID 83844, USA

ABSTRACT

Climate change may impact soil health and productivity as a result of accelerated or decelerated rates of erosion. Previous studies suggest a greater risk of wind erosion on arid and semi-arid lands due to loss of biomass under a future warmer climate. There have been no studies conducted to assess the impact of climate change on wind erosion in the Columbia Plateau of the Pacific Northwest United States where wind erosion of agricultural lands can cause exceedance of national air quality standards. The Wind Erosion Prediction System (WEPS) was used to assess wind erosion and PM10 (particulate matter $\leq 10\ \mu m$ in aerodynamic diameter) emissions under a future climate projected by downscaling 18 Global Climate Models (GCM) for a conservative emissions pathway. Wind erosion simulations were conducted at Lacrosse and Lind, WA and Moro, OR on a winter wheat-summer fallow (WW-SF) rotation and at Lind on an additional winter wheat-camelina-summer fallow (WW-Cam-SF) rotation. Each rotation was subject to conservation or conventional tillage practices for a baseline (1970–1999) and mid-21st century climate (2035–2064). A significant increase in temperature and nominal increases in precipitation were projected by an ensemble of climate models for the Columbia Plateau by the mid-21st century. Soil and PM10 losses were 25–84% lower for a mid-21st century climate, due in part to greater biomass production associated with CO_2 fertilization and warmer temperatures. The reduction in soil and PM10 loss is projected to be more apparent for conservation tillage practices in the future. Soil and PM10 losses were greater from a WW-Cam-SF rotation than WW-SF rotation when conservation tillage practices were employed during the fallow phase of the rotations. Despite accounting for differences in the length of each rotation, annual soil and PM10 losses remained higher for the WW-Cam-SF rotation than the WW-SF rotation. Soil and PM10 losses were more variable across years during 1970–1999 than 2035–2064; however, small and inconsistent differences in the coefficient of variation in soil loss between 1970–1999 and 2035–2064 suggest similarity in climate extremes which govern wind erosion.

Published by Elsevier B.V. This is an open access article under the CC BY-NC-ND license (http://creativecommons.org/licenses/by-nc-nd/4.0/).

1. Introduction

An increase in atmospheric concentrations of greenhouse gases and expected accompanying changes in temperature and precipitation may affect ecosystem health and human activities in the future. Indeed, the current function and structure of ecosystems may be unable to adapt in the 21st century as a result of changes in climate, land use, and exploitation of resources (IPCC, 2007). Human activities will be impacted by rising sea levels and coastal erosion and in areas where biological, geological, and hydrological resources are most sensitive to climate change or extreme weather events. Changes in hydrology could impact human activities in regions where freshwater supplies are continually replenished by ice and snow melt. These freshwater supplies are vulnerable owing to the rapid decline in number and size of glaciers worldwide (World Glacier Monitoring Service, 2008).

Climate change may also impact soil health and productivity. Wind erosion is of concern in arid and semi-arid regions of the world and escalates during drier years (Hagen and Woodruff, 1973). The impact of climate change on wind erosion, however, is difficult to assess owing to the complexity of predicting changes in climate, soil properties, and surface characteristics that govern erosion. Changes in temperature and precipitation can directly affect soil water content and crop production. For example, higher temperatures or lower precipitation can result in drier soils and limit crop production. Agricultural soils which are drier or more exposed, as a result of lower crop residue cover, are more prone to wind erosion (Fryrear, 1985; Sharratt et al., 2013). Wind speeds

associated with a changing climate are also of fundamental importance in assessing the impact of climate change on wind erosion. Yet, near-surface wind speeds are very difficult to model under a changing climate due to the limitations of regional climate models (Goyette et al., 2003), scaling (Pryor et al., 2006), and available data (Pryor et al., 2009). Advances in our understanding and simulation of the earth–atmosphere system in response to human activities or natural events and of dynamic changes in soil properties and surface characteristics caused by man or naturally will aid in assessing the impact of climate change on wind erosion.

Several studies have assessed the impact of climate change on wind erosion around the world. In Asia, Gao et al. (2002) predict that wind erosion of grassland will increase by about 25% as temperatures increase by 2 °C. They further predict that the increase in annual wind erosion will likely be more pronounced in the western part of Yijinhuoluo County in Inner Mongolia of China due to the soils being sandier in the western than eastern part of the County. In Australia, Liddicoat et al. (2012) predict greater risk for wind erosion of agricultural lands based upon a 5–20% reduction in precipitation, increase in CO_2 concentration from 390 to 480 ppm, and 1.5 °C increase in temperature by 2030 compared to the present climate. The greater risk of erosion was associated with the loss of critical biomass cover on an additional 335,000 (5% of arable land), 439,000 (6% of arable land), and 997,000 ha (15% of arable land) in response to a respective 5%, 10% or 20% reduction in precipitation across South Australia. Ashkenazy et al. (2011) also report a greater potential for drift of sand dunes in the Australian deserts by the mid- to late-21st century compared to the present due to lower precipitation and loss of vegetative cover under a changing climate. In Canada, Lemmen et al. (1997) used peleoenvironmental indicators to assess the response of eolian systems to climate. Based upon that response, they suggest enhanced wind erosion activity under a future warmer climate in the southern Canadian Prairies. In Europe, Böhner et al. (2004) used the Wind Erosion on European Light Soils (WEELS) model to assess the impact of climate change on wind erosion. They predict, from past climate anomalies in England, extended periods of erosion at the time of sowing spring crops in the future. The European Environment Agency (2012) also report that increased aridity and occurrence of extreme wind speeds will enhance wind erosion of fine-texture soils, particularly across central Europe. In the United States, Lee et al. (1996) predict an increase in wind erosion of cropland in the future. Wind erosion is estimated to increase by about 10–15% under higher atmospheric CO_2 concentrations (350 versus 625 ppm) and a warmer (2 °C higher air temperature) and wetter or drier (10% higher or lower precipitation) climate across the Corn Belt. In a later study, Lee et al. (1999) predicted wind erosion will increase four-fold at many locations across the Corn Belt under a future climate in which there was no change in temperature, precipitation or CO_2, but wind speeds were 20% higher as compared with the current climate. Likewise, Munson et al. (2011) projected an increase in dust storm activity as a result of enhanced aridity and loss of vegetation cover from grasslands in the Colorado Plateau of the southwestern United States.

There have been no studies conducted to assess the impact of climate change on wind erosion in the Columbia Plateau of the Pacific Northwest United States. Yet, air quality in this region is affected by wind erosion of agricultural lands. Wind erosion is a concern on approximately 2.5 million ha managed in a winter wheat-summer fallow (WW-SF) rotation. The soil is very susceptible to erosion during the fallow phase of the rotation because tillage-based summer fallow degrades aggregates and reduces biomass cover (Sharratt et al., 2012). Tillage-based fallow, however, is the most economical method of managing soils, especially in the low precipitation zone of the Columbia Plateau (Schillinger and Young, 2004). Nearly all exceedances of the PM10 National

Ambient Air Quality Standard are due to windblown dust emanating from agricultural lands (Sharratt and Lauer, 2006). Despite the lack of information on the effect of climate change on wind erosion, Thomson et al. (2002) predict an increase in winter wheat yield of 25–60% throughout the Columbia Plateau in response to a future CO_2 concentration of 560 ppm and a warmer and wetter climate. Similarly, Stöckle et al. (2009) also predict an increase in winter wheat yield in the region due to CO2 fertilization and higher temperatures, the latter which promotes earlier maturity to avoid late season water stress. They predict an increase in wheat yield of 20% by 2040 and 30% by 2080 based upon future CO_2 concentrations of 600 ppm and a warmer and wetter climate. The predicted increase in biomass production associated with climate change may enhance biomass cover during the fallow phase of the rotation and reduce the risk of wind erosion in the region.

No definitive studies have been conducted to ascertain the impact of climate change on wind erosion in the Columbia Plateau region of the Pacific Northwest United States. The purpose of this study is to assess wind erosion and PM10 emissions from agricultural lands under a changing climate in the region.

2. Materials and methods

The WEPS was used to assess wind erosion and PM10 emissions under future climate scenarios. The model was developed for conservation planning and assessing annual soil loss from agricultural lands in the United States (Hagen, 1991) and has been used extensively in research around the world (Buschiazzo and Zobeck, 2008; Chen et al., 2014; Coen et al., 2004; Feng and Sharratt, 2007; Maurer and Gerke, 2011). The model simulates changes in crop and soil surface characteristics as well as soil physical and hydrologic properties in response to weather and field operations on a daily basis. The model is comprised of seven submodels: crop growth, residue decomposition, erosion, hydrology, management, soil, and weather. The crop and decomposition submodels simulate plant growth and residue decomposition, the erosion submodel simulates wind erosion, the hydrology submodel simulates changes in soil water content, the management submodel simulates changes in soil properties caused by farming operations, the soil submodel simulates changes in soil properties caused by natural processes, and the weather submodel simulates precipitation, radiation, temperature, and wind characteristics to drive processes in other submodels.

2.1. Region of interest

The WEPS was used to simulate the impact of climate change on wind erosion in the low (< 300 mm annually) and intermediate (300–380 mm annually) precipitation zones of the Columbia Plateau. There are 1.5 million ha in the low precipitation zone and 1 million ha in the intermediate precipitation zone utilized for dryland agricultural production. A WW-SF rotation is the conventional rotation used in both precipitation zones (Schillinger et al., 2006). Simulations were carried out at Lind, WA and Moro, OR in the low precipitation zone and at Lacrosse, WA in the intermediate precipitation zone (Fig. 1). These locations were chosen based upon availability of winter wheat yield data collected by Oregon State University and Washington State University as well as representing dryland agriculture in the southwestern, central, and eastern part of the Columbia Plateau. Selected characteristics at each location are given in Table 1.

2.2. Models

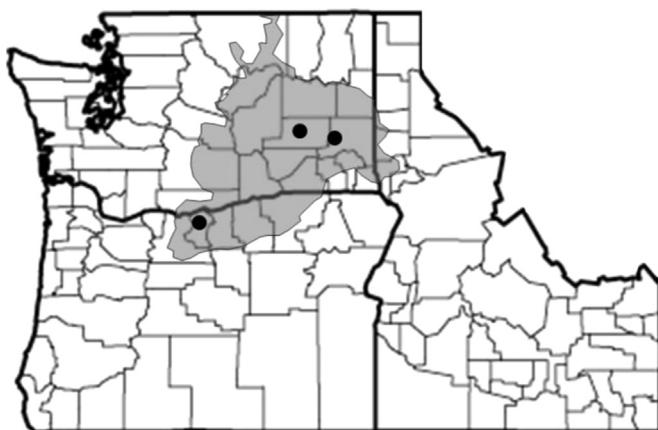Simulation of wind erosion was carried out over two 30-year

Fig. 1. Locations (solid circles) within the Columbia Plateau (shaded area) of northern Idaho, north-central Oregon, and eastern Washington where data were obtained in examining the impact of climate change on wind erosion.

periods, representative of historical baseline climate (1970–1999) and mid-21st century climate (2035–2064). These periods approximately represent those used by Thomson et al. (2002) and Stöckle et al. (2009) in simulating the impact of climate change on yield of winter wheat in the Columbia Plateau.

2.2.1. Climate

The WEPS requires input of daily maximum and minimum air temperature, relative humidity, solar radiation, and precipitation to simulate erosion. These inputs are used in the crop growth, residue decomposition, hydrology, management, soil, and weather submodels. Daily weather data were obtained from 18 Global Climate Models (GCM); those models included bcc-csm1-1, bcc-csm1-1-m, BNU-ESM, CanESM2, CNRM-CM5, CSIRO-Mk3-6-0, GFDL-ESM2G, GFDL-ESM2M, HadGEM2-CC365, HadGEM2-ES365, inmcm4, IPSL-CM5A-LR, IPSL-CM5A-MR, IPSL-CM5B-LR, MIROC5, MIROC-ESM, MIROC-ESM-CHEM, and MRI-CGCM3. These models participated in the fifth phase of the Climate Model Intercomparison Project (Taylor et al., 2012).

We use an ensemble approach for climate change impact assessment following the guidelines of Mote et al. (2011) as they consider intermodel variability of projected changes as a means of accounting for model uncertainty. These models were evaluated against observations across the northwestern United States using monthly temperature and precipitation data (Rupp et al., 2013). Daily GCM weather simulations that include wind speed, however, have not been evaluated in the region. Daily surface meteorological data at Lacrosse and Lind, WA and Moro, OR were obtained using co-located voxels from the 4-km gridded surface meteorological database of Abatzoglou (2013). These data included maximum and minimum air temperature, relative humidity, precipitation, shortwave radiation, and wind speed and have

demonstrated skill in capturing in-situ observations across the study area. The use of gridded weather data at such spatial (4 km) and temporal resolutions (daily) may be unable to capture true local-scale variations that arise across a landscape at sub-grid scale resolutions. However, we use these data to overcome many limitations of station observations that often have missing or poor quality data and may be affected by station siting including vegetation, infrastructure (e.g. urbanization) and topography.

Daily surface meteorological data were then used in tandem with daily output from GCM's to statistically downscale coarse resolution fields to the 4-km grid using the Multivariate Adapted Constructed Analogs method (Abatzoglou and Brown, 2012). Downscaling was performed for GCM simulations using both historical (1950–2005) and future forcings (2006–2099) at a Representative Concentration Pathway 4.5. Statistical downscaling has many limitations, but was preferred over using regional climate models (RCM) due to the limited availability of RCM runs that restrict ensemble analysis and potential biases in RCM output that inhibit direct application for additional modeling. In addition, downscaling of GCM weather data typically underestimates the occurrence of extreme events.

The WEPS also requires input of hourly wind speed and daily wind direction to simulate wind erosion with the erosion submodel. Since hourly wind speed and daily wind direction were not estimated by the GCM's, hourly wind speed and direction were generated using the weather simulator "WINDGEN" in WEPS. WINDGEN stochastically simulates hourly wind speed distributions with a daily maximum and minimum as well as a wind direction for the day that reflect historic wind distributions. These wind speed distributions were adjusted to give the same mean daily wind speeds obtained from the GCM's. Further details concerning the simulation of hourly wind speed and daily wind direction using WINDGEN can be found in van Donk et al. (2005).

2.2.2. Wind erosion

Although there is a lack of historic data to validate the performance of WEPS in simulating annual soil loss in the Columbia Plateau, Feng and Sharratt (2007) found an acceptable level of performance in using WEPS to simulate soil and PM10 loss during singular high wind events in eastern Washington. An acceptable level of performance in using WEPS to simulate erosion was also found in Argentina (Buschiazzo and Zobeck, 2008), Germany (Funk et al., 2004), and other regions of the United States (Hagen, 2004). These observations provided confidence in using WEPS to simulate erosion for historic and future climates.

The WEPS simulates erosion at field scales. Our simulations were performed on a rectangular field having a typical dimension of 1610×805 m² (about 130 ha) with the longer dimension oriented north-south and in the direction of field tillage operations and perpendicular to the prevailing winds. The field dimensions ensured attainment of transport capacity for estimating PM10 and

Table 1
Select characteristics of three locations where the Wind Erosion Prediction System was used to simulate the impact of climate change on wind erosion and PM10 emissions.

Location	Coordinates	Annual[a]		Major soils	Cover (%)[b]
		Precipitation (mm)	Temperature (°C)		
Lacrosse, WA	46°49′N, 117°53′W	380	10.1	Walla Walla silt loam	70
Lind, WA	47°00′N, 118°34′W	250	9.9	Ritzville silt loam	50
				Shano silt loam	30
Moro, OR	45°29′N, 120°44′W	290	9.6	Condon silt loam	15
				Walla Walla silt loam	50

[a] Obtained from National Climatic Data Center website http://www.ncdc.noaa.gov/cdo-web/datatools/normals.
[b] Cover represents the approximate area occupied by the given soil within a 40,000 ha area incorporating the location as determined using the USDA Natural Resource and Conservation Service soil database.

Table 2

Crop rotations and tillage practices employed at Lacrosse, WA; Lind, WA; and Moro, OR for simulating the impact of climate change on wind erosion using the Wind Erosion Prediction System.

Rotation	Tillage	Field operations	Date of field operation		
			Lacrosse	Lind	Moro
WW-SF[a]	Conventional	Harvest wheat	August 1	July 15	July 15
		Sweep tillage	August 30	August 15	August 15
		Herbicide application	February 15	February 20	February 20
		Disk tillage	March 15	March 20	March 20
		Fertilizer application	April 15	April 15	April 15
		Rodweed	May 15	May 15	May 15
		Rodweed	June 15	June 15	June 15
		Rodweed	July 15	July 15	July 15
		Sow wheat	September 15	September 1	September 1
	Conservation	Harvest wheat	August 1	July 15	July 15
		Herbicide application	August 30	August 15	August 15
		Herbicide application	February 20	February 20	February 20
		Undercutter tillage	May 15	May 15	May 20
		Rodweed	June 15	June 15	June 15
		Rodweed	July 15	July 15	July 15
		Sow wheat	September 15	September 1	September 1
WW-Cam-SF[b]	Conservation	Harvest wheat	NA[c]	July 15	NA
		Herbicide application	NA	August 15	NA
		Fertilization application	NA	February 15	NA
		Sow camelina	NA	March 1	NA
		Herbicide application	NA	April 1	NA
		Harvest camelina	NA	July 15	Na
		Herbicide application	NA	August 15	NA
		Herbicide application	NA	February 20	NA
		Undercutter tillage	NA	May 15	NA
		Rodweed	NA	June 15	NA
		Rodweed	NA	July 15	NA
		Sow wheat	NA	September 1	NA

[a] Winter wheat-summer fallow.
[b] Winter wheat-camelina-summer fallow.
[c] Not applicable.

total soil loss. Total soil loss is derived from loss associated with creep, saltation, and suspension whereas PM10 loss is a subset of the suspension component in WEPS.

2.2.2.1. Crop and soil management. The WEPS requires information about crop and soil management practices for simulating changes in crop growth and residue characteristics and soil physical properties and surface characteristics. Crop rotations and tillage practices employed at Lacrosse, WA; Lind, WA; and Moro, OR are presented in Table 2. Wind erosion was simulated for a WW-SF rotation using both conventional and conservation tillage practices at the three locations as well as for a winter wheat-camelina-summer fallow (WW-Cam-SF) rotation using conservation tillage at Lind, WA. The WW-Cam-SF rotation was of interest due to recent attempts at incorporating biofuel crops into the conventional WW-SF rotation (Wysocki et al., 2013). Briefly, conventional tillage includes sweeping or disking in August after harvest of wheat and the following spring and then rodweeding during the summer months prior to sowing wheat in early to mid-September. Conservation tillage includes applying herbicides to control weeds after harvest of wheat and prior to using an undercutter in the spring and then rodweeding twice during summer prior to sowing wheat. Conventional and conservation field operations performed in WW-SF rotations are outlined by Schillinger et al. (2006) whereas conservation field operations performed in WW-Cam-SF rotations are outlined by Sharratt and Schillinger (2014).

The crop and decomposition submodels in WEPS were calibrated based upon a winter wheat grain yield of 6390 kg ha^{-1} at Lacrosse, WA; 3025 kg ha^{-1} at Lind, WA; and 5045 kg ha^{-1} at

Moro, OR for 1970–1999. These grain yields represent those currently obtained from varietal trials conducted at the respective locations by Oregon State University and Washington State University. During calibration, WEPS adjusts crop growth parameters in iterative steps until the average grain yield is within 5% of the expected yield. Once grain yield is within 5% of the expected yield, the resultant crop growth parameters are subsequently used in simulating wind erosion from a WW-SF rotation. The crop and decomposition submodels were also calibrated for a winter wheat grain yield of 7670 kg ha^{-1} at Lacrosse, WA; 3630 kg ha^{-1} at Lind, WA; and 6055 kg ha^{-1} at Moro, OR for 2035–2064. These yields represent a 20% increase from 1970–1999 to 2035–2064 as nearly projected by Thomson et al. (2002) and Stöckle et al. (2009). The range in wheat yield simulated by WEPS for the WW-SF rotation at Lacrosse, Lind, and Moro was respectively 5150–7120, 1890–4040, and 3410–6980 kg ha^{-1} during 1970–1999 and 6190–8560, 2440–4860, and 4160–8140 kg ha^{-1} during 2035–2064. This range in wheat yield is in response to variations in climate projected by the 18 GCM's. Crop growth parameters were determined in a similar manner for camelina based upon a grain yield of 500 and 600 kg ha^{-1} at Lind, WA for respectively 1970–1999 and 2035–2064; the former grain yield represents that currently obtained from trials conducted at Lind (Schillinger et al., 2012). The range in camelina yield simulated by WEPS for the WW-Cam-SF rotation at Lind was 210–1010 kg ha^{-1} during 1970–1999 and 290–1320 kg ha^{-1} during 2035–2064. We assumed that 50% of the standing stubble remained after harvest of wheat and camelina and that dead weeds from herbicide applications did not contribute to flat residue cover.

3. Results and discussion

Climate data generated by the 18 GCM's were used in our analysis of the impact of climate change on wind erosion. Our analysis was not restricted to a subset of these GCM's used by the IPCC (2013), even though significant biases exist among these models. Mote et al. (2011) recommended using projections from an ensemble of GCM's for characterizing the future climate. Therefore, wind erosion simulations based upon climate data from each of the 18 models were used to assess the potential variability of the future climate and the impact of climate change on wind erosion.

An ensemble of 18 GCM's suggest a warmer climate throughout the Columbia Plateau of the Inland Pacific Northwest United States during 2035–2064 than 1970–1999 (Fig. 2). Air temperatures are higher throughout the year during 2035–2064 with the greatest change occurring during summer and winter. These models also project a slightly wetter climate throughout the Columbia Plateau during 2035–2064 than 1970–1999 (Fig. 3). Annual precipitation is projected to be higher during 2035–2064 with winters being

wetter and summers being drier compared to 1970–1999. A small or negligible reduction is projected to occur in wind speed across the Columbia Plateau in the future (Fig. 4). For the three locations considered in this study, annual air temperature is projected to be ≥ 2 °C higher in 2035–2064 than 1970–1999 based upon an ensemble of the 18 GCM's (Table 3). Seasonal temperature changes are projected to be highest during summer (2.5 °C) and lowest during autumn and spring (about 2 °C). Annual precipitation at the three locations is projected to be about 5% greater in 2035–2064 than 1970–1999. Autumn, winter, and spring are likely to be wetter and summer drier in 2035–2064 at each location. A small reduction in seasonal wind speed is projected for the three locations. The reduction in wind speed is projected to occur primarily during summer at Lacrosse and Lind, WA and during autumn at Moro, OR. Seasonal wind speeds are projected to be lower by 1.1–2.1% at Lacrosse, WA; 1.3–2.5% at Lind, WA; and 1.2–2.1% at Moro, OR during 2035–2064 than 1970–1999.

Future projections of climate varied across the 18 GCM's (data not shown). For example, although all models projected an increase in annual air temperature at the three locations from 1970–
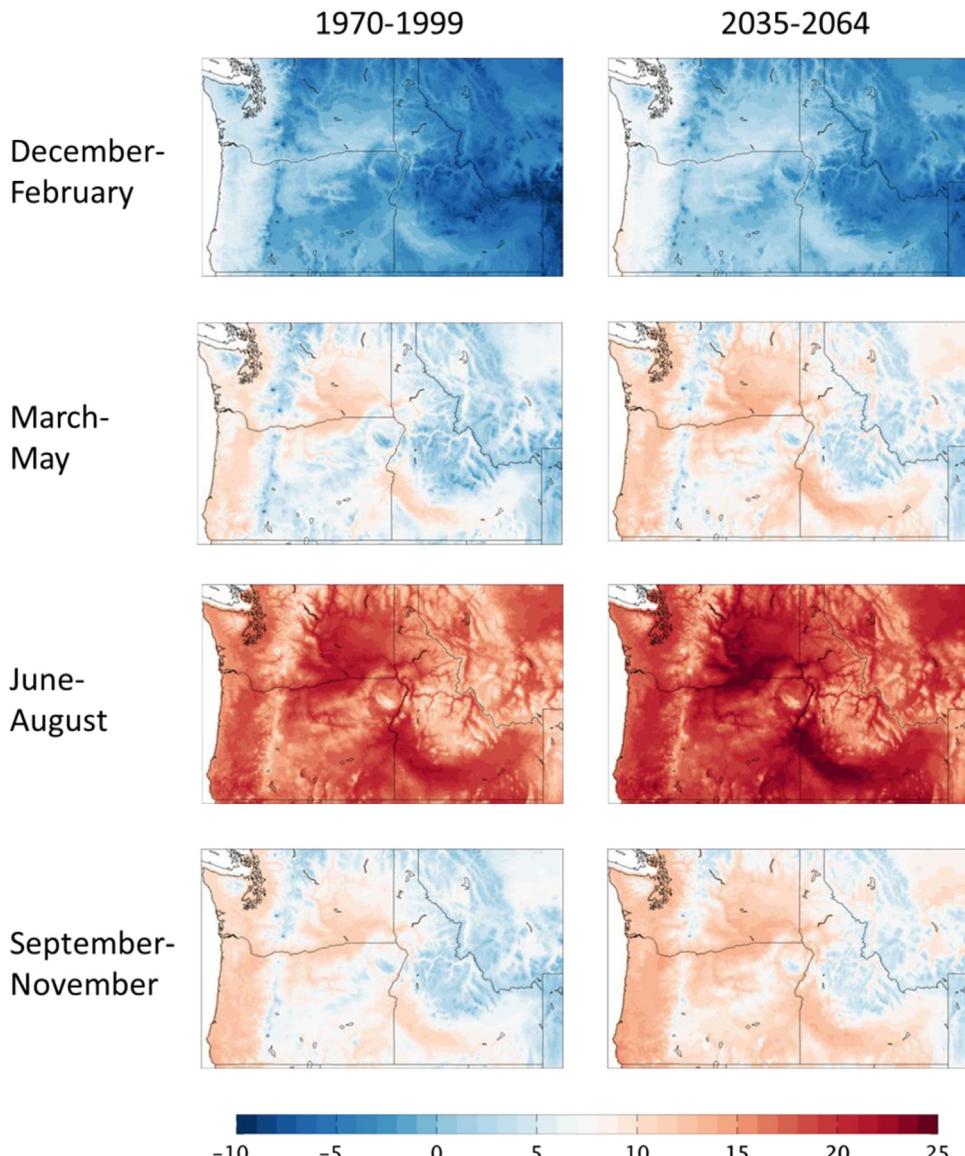

Fig. 2. Seasonal average air temperature (°C) across Idaho, western Montana, Oregon, and Washington averaged over 18 Global Climate Models using historical and Representative Concentration Pathway 4.5 forcing for respectively 1970–1999 and 2035–2064. Air temperature is reported for winter (December–February), spring (March–May), summer (June–August) and autumn (September–November).
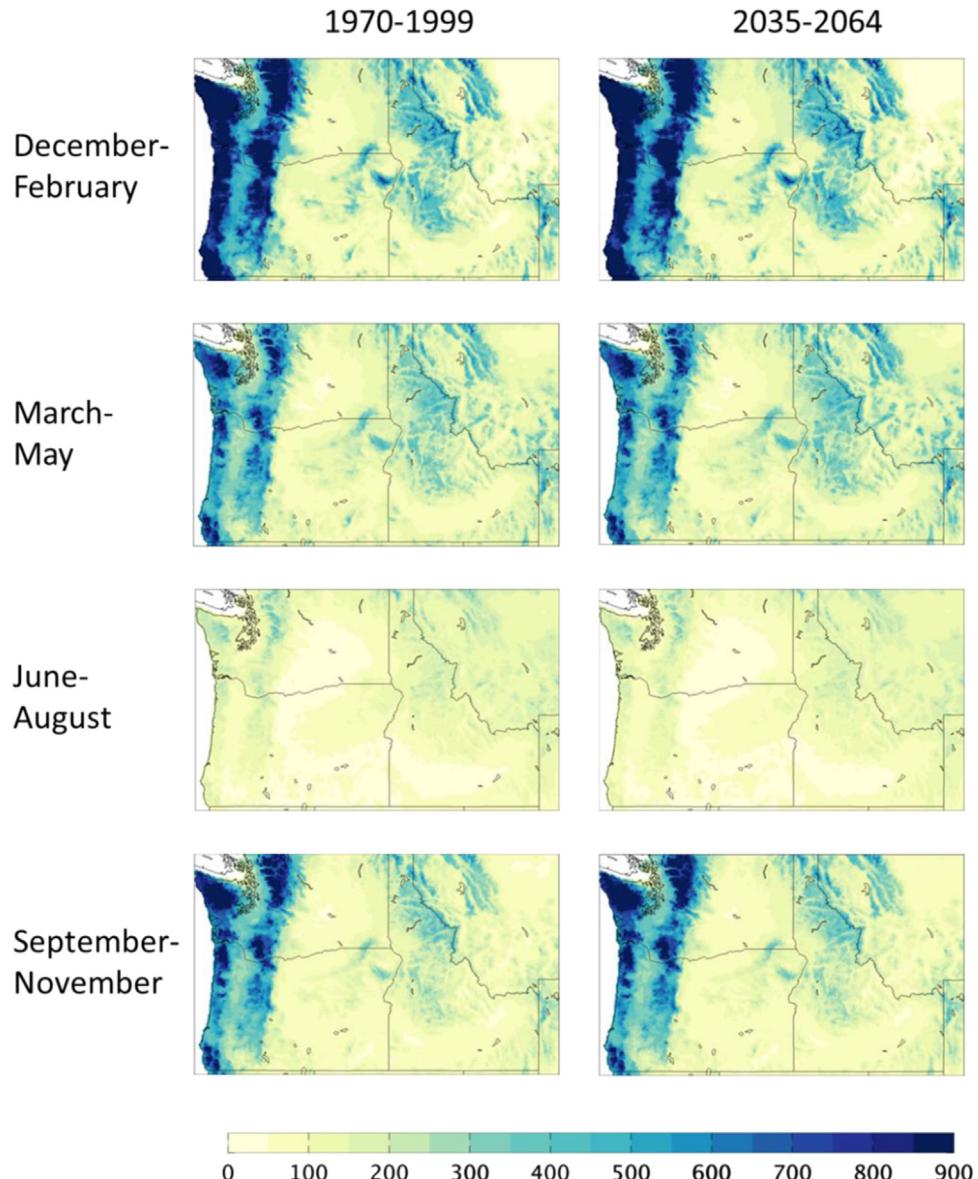
Fig. 3. Total seasonal precipitation (mm) across Idaho, western Montana, Oregon, and Washington averaged over 18 Global Climate Models using historical and Representative Concentration Pathway 4.5 forcing for respectively 1970–1999 and 2035–2064. Precipitation is reported for winter (December–February), spring (March–May), summer (June–August) and autumn (September–November).

1999 to 2035–2064, the increase in air temperature was $>3.0\,°C$ using the MIROC-ESM-CHEM model and $<1.1\,°C$ using the GFDL-ESM2M and inmcm4 models. The largest increase in air temperature projected by the MIROC-ESM-CHEM model occurred in spring $(3.6\,°C)$ at Lacrosse and Lind, WA and in summer $(3.8\,°C)$ at Moro, OR while the largest increase in air temperature projected by the GFDL-ESM2M and inmcm4 models occurred respectively in spring $(1.0–1.6\,°C)$ and summer $(1.3–1.4\,°C)$ across the three locations. The 18 GCM's varied greatly in projecting change in annual precipitation from 1970–1999 to 2035–2064. While most GCM's projected an increase in precipitation, the ISPL-CM5A-LR, ISPL-CM5A-MR, MIROC-ESM, and MIROC-ESM-CHEM models projected a decrease in precipitation at one or more locations. The MIROC-ESM-CHEM model projected the greatest decrease in precipitation (6 mm at Lacrosse, WA; 8 mm at Lind, WA; and 28 mm at Moro, OR). In contrast, the greatest increase in precipitation was projected by the GFDL-ESM2G model at Lacrosse (49 mm) and Lind, WA (34 mm) and by the ISPL-CM5B-LR model at Moro, OR (32 mm). Most GCM's projected a small decrease $(<2\%)$ in annual

wind speed from 1970–1999 to 2035–2064. In fact, 13 and 14 GCM's projected a decrease in wind speed at respectively Lacrosse, WA and Lind, WA and Moro, OR. The MIROC-ESM-CHEM model projected the most significant decrease in wind speed at the three locations (12% at Lacrosse and Lind, WA and 7% at Moro, OR). Of the GCM's that projected an increase in annual wind speed, the bcc-csm1-1 and CNRM-CM5 models projected a $<1\%$ increase in wind speed across the three locations.

Specific GCM's also exhibited unique climatic features common across the three locations. For example, the MIROC5 model simulated the lowest autumn, spring, summer, and winter temperatures during 1970–1999 while the inmcm4 model simulated the lowest autumn and spring temperatures during 2035–2064. In addition, the ISPL-CM5A-LR model simulated the wettest autumns and summers during 1970–1999 while the MIROC-ESM-CHEM model simulated the driest autumns and springs during 2035–2064. There was little variation in simulated seasonal wind speeds across all GCM's during 1970–1999; however, the MIROC-ESM-CHEM model simulated the lowest autumn, spring, and winter
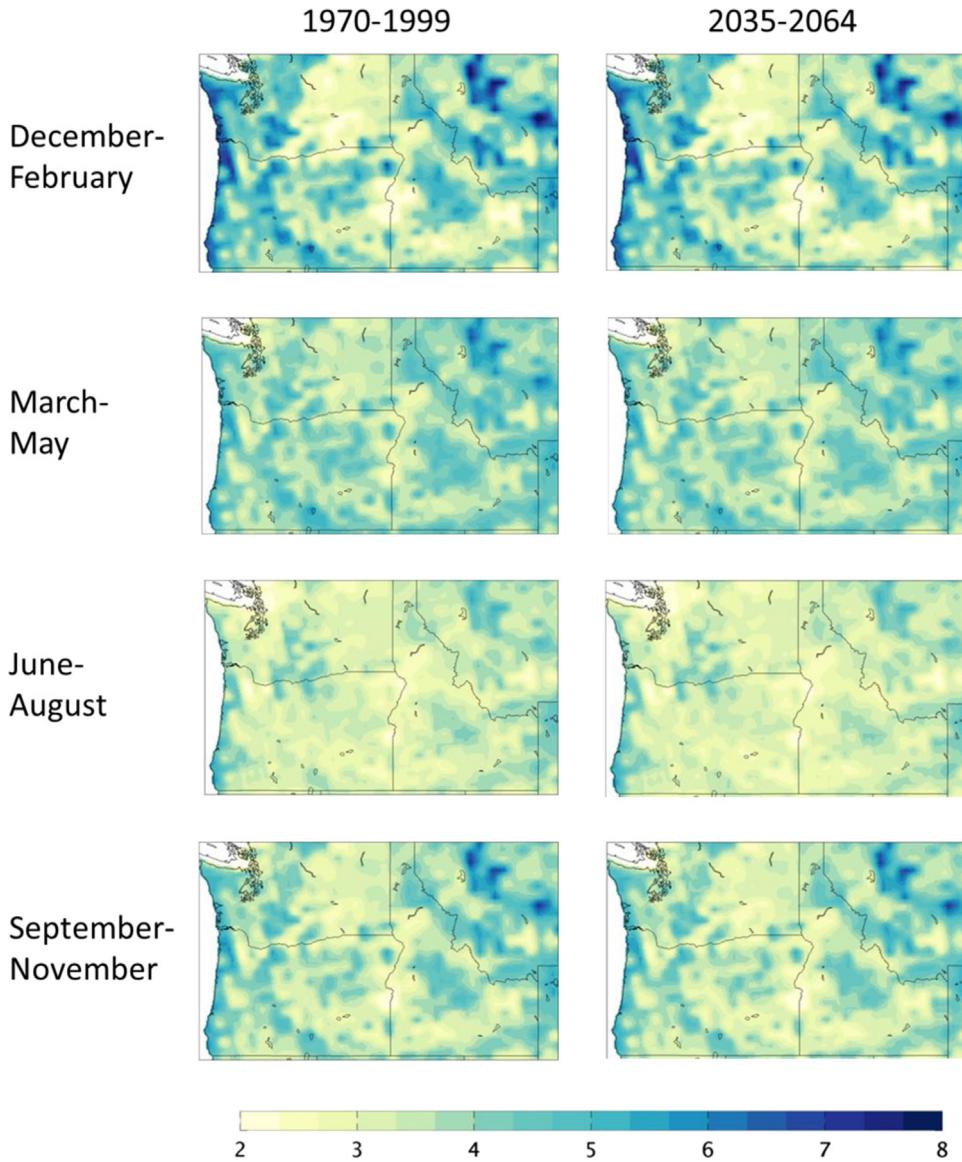
Fig. 4. Seasonal average wind speed (m s^{-1}) across Idaho, western Montana, Oregon, and Washington averaged over 18 Global Climate Models using historical and Representative Concentration Pathway 4.5 forcing for respectively 1970–1999 and 2035–2064. Wind speed is reported for winter (December–February), spring (March–May), summer (June–August) and autumn (September–November).

wind speeds during 2035–2064.

Soil and PM10 losses simulated by WEPS are projected to decrease in 2035–2064 compared to 1970–1999 (Table 4). This reduction in soil and PM10 loss is significant ($P=0.05$) for all soils, tillage practices, and cropping systems at the three locations, except for conservation tillage in a WW-SF rotation at Lacrosse, WA. The decrease in soil loss ranges from 25% using conventional tillage in a WW-SF rotation at Lacrosse, WA to 84% using conservation tillage in a WW-SF rotation at Moro, OR. Similarly, the decrease in PM10 loss ranges from 30% using conventional tillage in a WW-SF rotation at Lacrosse, WA to nearly 82% using conservation tillage in a WW-SF rotation at Moro, OR. Soil and PM10 losses from the WW-Cam-SF rotation are comparable to losses from the WW-SF rotation subject to conventional tillage at Lind, WA. When conservation tillage practices are utilized in both the WW-Cam-SF and WW-SF rotations, however, soil and PM10 losses are at least 25 and 40 times higher from the WW-Cam-SF rotation during respectively 1970–1999 and 2035–2064. These results suggest that camelina or other oilseed crops introduced into the conventional WW-SF rotation in the low precipitation zone of the Columbia

Plateau may have deleterious effects on soil erosion. Soil and PM10 losses for the WW-Cam-SF rotation in Table 4 is the cumulative over the three year rotation whereas losses for the WW-SF rotation are the cumulative over the two year rotation. Despite accounting for the difference in length of each rotation, average annual soil and PM10 losses remain higher for the WW-Cam-SF rotation than the WW-SF rotation. In fact, average annual soil and PM10 losses are at least 15 and 25 times higher from the WW-Cam-SF rotation than the WW-SF rotation during respectively 1970–1999 and 2035–2064. This concurs with Sharratt and Schillinger (2014) who found that sediment and PM10 flux were at least 200% higher after sowing wheat in the WW-Cam-SF rotation than the WW-SF rotation. Thus, the results suggest the need for even more stringent conservation practices than those implemented in this study when introducing camelina into WW-SF rotations to reduce the risk of wind erosion in the region.

The impact of climate change on wind erosion was also examined assuming no change in crop biomass production between 1970–1999 and 2035–2064. Assuming biomass production of winter wheat and camelina does not change over time, soil and

Table 3
Recent and future climate simulated by Global Climate Models (GCM) at Lacrosse, WA; Lind, WA; and Moro, OR. The simulations were performed over 1970–1999 and 2035–2064 with results averaged over 18 GCM.

Climate parameter	Location					
	Lacrosse		Lind		Moro	
	1970–1999	2035–2064	1970–1999	2035–2064	1970–1999	2035–2064
Precipitation, total (mm)						
December–February	137	147	83	90	109	117
March–May	105	113	69	75	76	78
June–August	44	42	33	32	29	29
September–November	90	95	66	70	79	82
Temperature, mean (°C)						
December–February	0.4	2.7	−0.1	2.2	0.6	2.6
March–May	9.8	11.8	10.0	12.1	9.0	10.8
June–August	19.9	22.5	20.3	22.8	18.8	21.3
September–November	9.8	11.8	10.0	12.0	9.8	11.7
Wind speed, mean (m s^{-1})						
December–February	2.8	2.8	2.3	2.2	3.6	3.6
March–May	3.5	3.4	3.0	3.0	4.1	4.1
June–August	3.3	3.2	2.8	2.8	4.2	4.1
September–November	3.1	3.1	2.7	2.6	3.8	3.7

PM10 loss are projected to decrease during 2035–2064 as compared with 1970–1999 at all locations except Lacrosse, WA. For example, soil loss occurring during the WW-SF rotation using conventional tillage on Ritzville silt loam at Lind, WA is projected to be 11579 kg ha^{-1} in 2035–2064 as compared to 30257 kg ha^{-1} in 1970–1999. Similarly, soil loss occurring during the WW-SF rotation using conventional tillage on Walla Wall silt loam at Moro, OR is projected to be 9225 kg ha^{-1} in 2035–2064 as compared to 16455 kg ha^{-1} in 1970–1999. In contrast, soil loss occurring during the WW-SF rotation using conventional tillage at Lacrosse, WA is projected to be 49026 kg ha^{-1} in 2035–2064 as compared to 38348 kg ha^{-1} in 1970–1999. We anticipated greater wind erosion in 2035–2064 as a result of less biomass production under a warmer future climate (in the absence of CO_2 fertilzation), but lower seasonal wind speeds and higher precipitation may contribute to the decline in wind erosion from 1970–1999 to 2035–2064 at Lind, WA and Moro, OR.

The impact of climate change on wind erosion, driven in part by changes in crop production, is projected to be more apparent at drier than at wetter locations in the Columbia Plateau. For example, the reduction in soil loss using conventional tillage in a WW-SF rotation is projected to be about 72% at Lind, WA; 64% at Moro, OR; and 25% at Lacrosse, WA while the reduction in PM10 loss using conventional tillage in a WW-SF rotation is projected to be about 74% at Lind, WA; 65% at Moro, OR (i.e. low precipitation zone); and 31% at Lacrosse, WA (i.e. intermediate precipitation zone). Similar reductions in soil and PM10 losses were found at the respective locations using conservation tillage in a WW-SF rotation. The larger reduction in soil and PM10 loss from 1970–1999 to 2035–2064 at drier locations is likely due to the influence of biomass production on wind erosion processes. Although crop yield is projected to increase by 20% across the Columbia Plateau (Stöckle et al., 2009; Thomson et al., 2002), this projected increase may have a larger impact on wind erosion at locations with lower biomass production as wind erosion varies exponentially with crop residue biomass. For example, Hagen (1996) observed an exponential increase in wind erosion as crop residue cover decreased from about 50–0%. Bilbro and Fryrear (1994) and Fryrear

Table 4
Soil and PM10 loss during summer fallow simulated by the Wind Erosion Prediction System for crop rotations and tillage practices employed at Lacrosse, WA; Lind, WA; and Moro, OR during 1970–1999 and 2035–2064. Soil and PM10 losses were simulated by WEPS using climate data from 18 Global Climate Models.

Location	Rotation[a]	Tillage	Soil	Loss[b] (kg ha^{-1})							
				Total soil				PM10			
				1970–1999		2035–2064		1970–1999		2035–2064	
				Mean	SE[c]	Mean	SE	Mean	SE	Mean	SE
Lacrosse	WW-SF	Conventional	Walla Walla	38,348	2025	28,582	1298	874	46	607	27
		Conservation	Walla Walla	369	33	263	23	9	1	6	1
Lind	WW-SF	Conventional	Ritzville	30,257	4743	8756	1180	1490	237	400	55
			Shano	29,867	4707	8229	1197	1472	236	376	55
		Conservation	Ritzville	1042	212	233	123	49	10	10	3
			Shano	996	209	222	118	47	10	10	3
	WW-Cam-SF	Conservation	Ritzville	26,621	5782	9572	1441	1314	286	434	66
			Shano	26,323	5806	9813	1449	1298	286	446	67
Moro	WW-SF	Conventional	Walla Walla	16,455	3011	5799	941	479	87	160	27
			Condon	8624	1355	3224	580	232	37	84	15
		Conservation	Walla Walla	388	115	62	15	11	3	2	1
			Condon	228	50	63	15	7	1	2	1

[a] WW-SF is winter wheat-summer fallow and WW-Cam-SF is winter wheat-camelina-summer fallow.
[b] Loss of soil and PM10 over the two or three year rotation.
[c] SE is standard error of mean across years with annual soil and PM10 loss determined from an ensemble of 18 Global Climate Models.
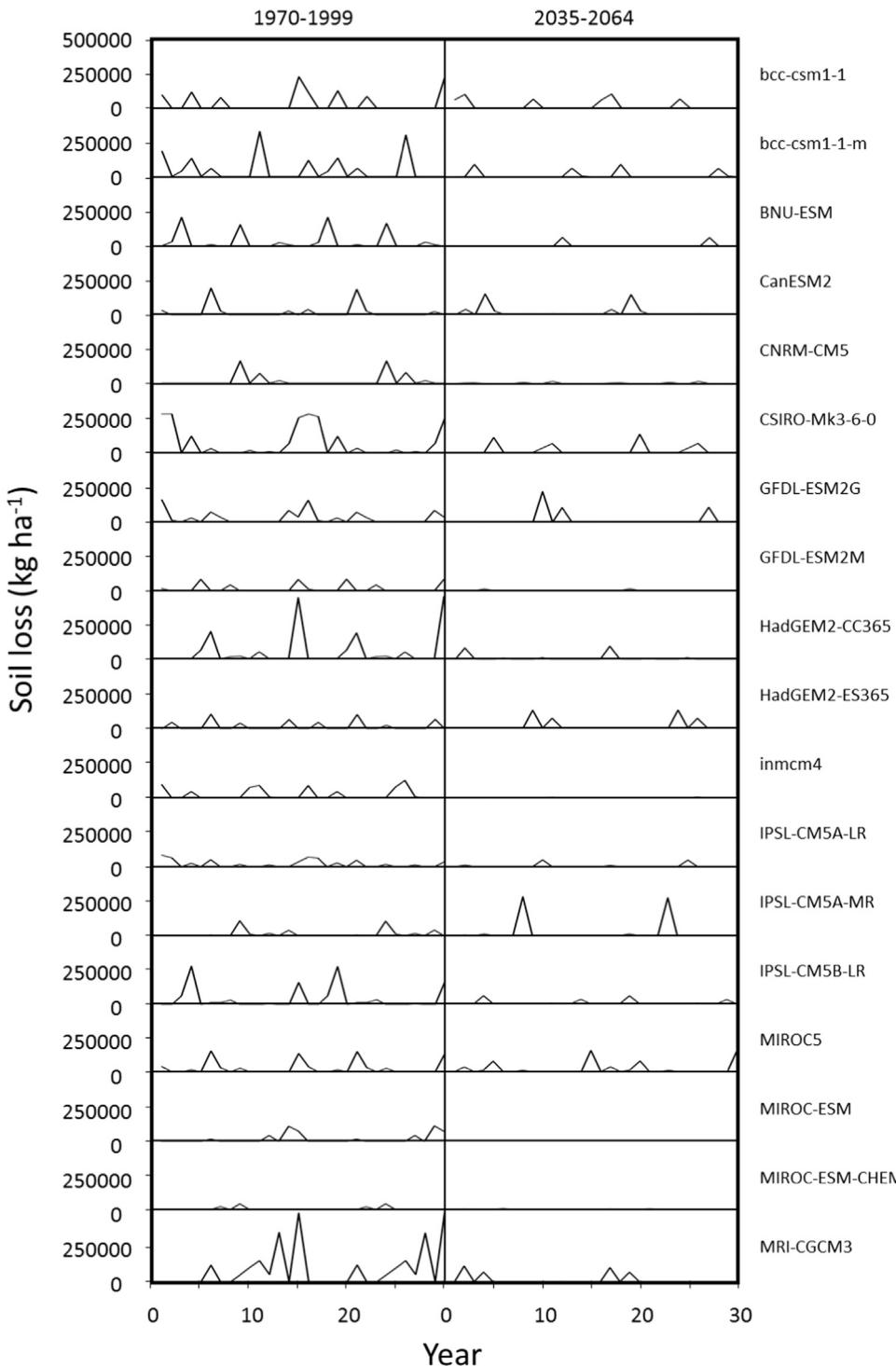
Fig. 5. Soil loss simulated by the Wind Erosion Prediction System across climates generated by 18 Global Climate Models for a winter wheat-summer fallow rotation on Ritzville silt loam subject to conventional tillage at Lind, WA. Annual soil loss is presented for the fallow phase of the rotation during 1970–1999 and 2035–2064 with each phase of the rotation simulated during the 30 years.

(1985) also reported higher soil loss occurring with lower surface residue cover. Thus, a small incremental change in biomass production, and therefore biomass cover, will have a larger influence on wind erosion at locations with lower crop yield.

The reduction in soil and PM10 loss is projected to be more apparent for conservation tillage practices in the future. For example, the reduction in soil and PM10 loss from 1970–1999 to 2035–2064 was greater for conservation tillage than conventional tillage in the WW-SF rotation at the three locations (Table 4). The

reduction in soil loss from 1970–1999 to 2035–2064 for conservation and conventional tillage in a WW-SF rotation is projected to be respectively 29% and 26% at Lacrosse, WA; 78% and 72% at Lind, WA; and 78% and 64% at Moro, OR. Similarly, the reduction in PM10 loss from 1970–1999 to 2035–2064 for conservation and conventional tillage in a WW-SF rotation is projected to be respectively 33% and 30% at Lacrosse, WA; 79% and 74% at Lind, WA; and 77% and 65% at Moro, OR. The greater reduction in soil and PM10 loss using conservation tillage may be
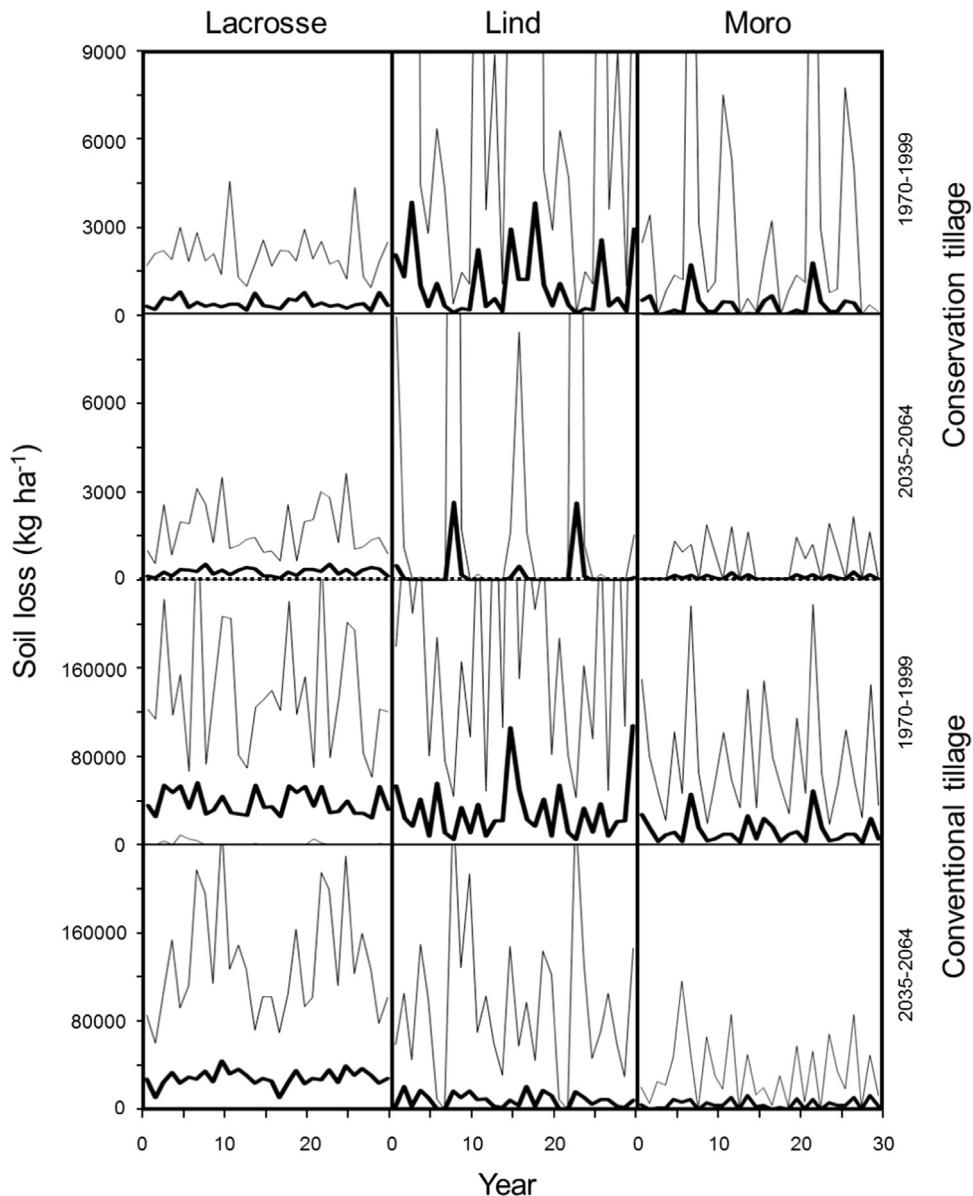
Fig. 6. Soil loss simulated by the Wind Erosion Prediction System (WEPS) for a winter wheat-summer fallow rotation at Lacrosse, WA; Lind, WA; and Moro, OR during 1970–1999 and 2035–2064. Annual soil loss is presented for the fallow phase of the rotation with each phase of the rotation simulated during the 30 years. Soil loss at Lind, WA and Moro, OR is an average across two soil types. Soil loss simulated by WEPS represents an average (thick line) and range (thin lines) of loss across climate projections by 18 Global Climate Models.

associated with the enhanced biomass production under a warmer and wetter climate and retention of crop residue on the soil surface using conservation tillage. Although a warmer and wetter climate overall should result in greater residue decomposition, the summers in 2035–2064 are projected to be drier than 1970–1999 which would result in less residue decomposition during that period. Sharratt et al. (2012) noted tillage intensity during summer fallow greatly influenced residue retention on the soil surface. Indeed, they found reduced tillage retained at least twice as much residue on the surface compared with conventional tillage at the end of the fallow phase of a WW-SF rotation in the Columbia Plateau.

Soil and PM10 losses simulated by WEPS are more variable across climates generated by the 18 GCM's during 2035–2064 than 1970–1999. The variation in soil loss simulated by WEPS across climates generated by the GCM's during 1970–1999 and 2035–2064 is illustrated in Fig. 5 for a WW-SF rotation on Ritzville silt loam subject to conventional tillage practices at Lind, WA.

Although the absolute variation (expressed as standard error or SE) in simulated soil and PM10 loss was typically greater across climates generated by the GCM's during 1970–1999 than 2035–2064 at the three locations, the relative variation (expressed as coefficient of variation or CV) in soil and PM10 loss was typically greater across climates generated by the GCM's during 2035–2064 than 1970–1999. For example, the SE in soil and PM10 losses simulated by WEPS was greater during 1970–1999 than 2035–2064, except for the WW-SF rotation using conventional tillage at Lacrosse, WA. At Lacrosse, the SE in soil loss simulated by WEPS across climates generated by the GCM's was 2505 kg ha^{-1} during 1970–1999 and 3294 kg ha^{-1} during 2035–2064 while the SE in PM10 loss was 57 kg ha^{-1} during 1970–1999 and 71 kg ha^{-1} during 2035–2064. The SE in soil loss simulated by WEPS across climates generated by the GCM's ranged from 49 kg ha^{-1} for the WW-SF rotation subject to conservation tillage at Lacrosse, WA to 5249 kg ha^{-1} for the WW-Cam-SF rotation on Ritzville silt loam at Lind, WA during 1970–1999 and from 17 to 3294 kg ha^{-1} for the

WW-SF rotation subject to respectively conservation tillage on a Condon silt loam at Moro, OR and conventional tillage at Lacrosse, WA during 2035–2064. Likewise, the SE in PM10 loss simulated by WEPS across climates generated by the 18 GCM's ranged from 1 kg ha^{-1} for the WW-SF rotation subject to conservation tillage at Lacrosse, WA to 262 kg ha^{-1} for the WW-Cam-SF rotation on Ritzville silt loam at Lind, WA during 1970–1999 and from 1 kg ha^{-1} for the WW-SF rotation subject to conservation tillage at both Lacrosse, WA and Moro, OR to 120 kg ha^{-1} for the WW-Cam-SF rotation on Shano silt loam at Lind, WA during 2035–2064. The CV in soil and PM10 loss simulated by WEPS across climates generated by the 18 GCM's was lowest for the WW-SF rotation subject to conventional tillage at Lacrosse, WA during both 1970–1999 and 2035–2064 and highest for the WW-SF rotation subject to conservation tillage on Walla Walla silt loam at Moro, OR during 1970–1999 and WW-SF rotation subject to conservation tillage at Lind, WA during 2035–2064. The CV in soil loss simulated by WEPS across climates of the 18 GCM's ranged from 27.7% for the WW-SF rotation subject to conventional tillage at Lacrosse, WA to 152.0% for the WW-SF rotation subject to conservation tillage on Walla Walla silt loam at Moro, OR during 1970–1999 and from 48.9% for the WW-SF rotation subject to conventional tillage at Lacrosse, WA to 328.7% for the WW-SF rotation subject to conservation tillage on Shano silt loam at Lind, WA during 2035–2064. Similarly, the CV in PM10 loss as simulated by WEPS across climates of the 18 GCM's ranged from 27.7% for the WW-SF rotation subject to conventional tillage at Lacrosse, WA to 154.3% for the WW-SF rotation subject to conservation tillage on Walla Walla silt loam at Moro, OR during 1970–1999 and from 49.6% for the WW-SF rotation subject to conventional tillage at Lacrosse, WA to 339.4% for the WW-SF rotation subject to conservation tillage at Lind, WA during 2035–2064. The greater CV in soil and PM10 loss during 2035–2064 may reflect more extreme variations in climate predictions, or climatic parameters which govern wind erosion, across the 18 GCM's during 2035–2064 than 1970–1999.

The ranking in soil and PM10 losses simulated by WEPS based upon climate projections from the 18 GCM's varied by location, tillage, and time (data not shown). At Lacrosse, WA, soil and PM10 losses from conservation and conventional tillage during 1970–1999 and 2035–2064 were greatest based upon climate projections from MRI-CGCM3 or MIROC5 and typically smallest based upon climate projections from bcc-csm1-1, bcc-csm1-1-m, or IPSL-CM5A-MR. At Lind, WA, soil and PM10 losses from conservation and conventional tillage during 1970–1999 were typically greatest and smallest based upon climate projections from respectively MRI-CGCM3 and MIROC-ESM-CHEM (Fig. 5). Soil and PM10 losses from conservation and conventional tillage during 2035–2064, however, were typically greatest and smallest based upon climate projections from respectively IPSL-CM5A-MR and MIROC-ESM (Fig. 5). At Moro, OR, soil and PM10 losses from conservation and conventional tillage during 1970–1999 were typically greatest and smallest based upon climate projections from respectively MRI-CGCM3 and HadGEM2-CC365. Soil and PM10 losses from conservation and conventional tillage during 2035–2064, however, were typically greatest and smallest based upon climate projections from respectively bcc-csm1-1-m and IPSL-CM5B-LR. While tillage (conservation versus conventional) and time (1970–1999 versus 2035–2064) influenced the ranking in soil and PM10 losses associated with climate projections of the 18 GCM's, the ranking in soil and PM10 loss simulated by WEPS based upon the climate projections from the GCM's did not vary for the two soil types at Lind, WA or Moro, OR.

Trends in annual soil loss for a WW-SF rotation at the three locations during 1970–1999 and 2035–2064 are presented in Fig. 6. Annual soil loss portrayed in Fig. 6 is an average and range of WEPS simulations performed using climate projections from each of the 18 GCM's. The trends represent soil loss during the summer fallow phase of the rotation with each phase of the rotation simulated by WEPS every year. No soil loss was simulated by WEPS during the wheat phase of the rotation. The upper and lower range in annual soil loss among the WEPS simulations using climate projections from the 18 GCM's is not always apparent in Fig. 6. Nevertheless, the lower range in annual soil loss was 0 kg ha^{-1} across all locations, tillage practices, and years except for conventional tillage during 1970–1999 and 2035–2064 at Lacrosse, WA and for conventional tillage during 1970–1999 at Moro, OR. The lower range in annual soil loss approached 9300 and 1600 kg ha^{-1} for conventional tillage during respectively 1970–1999 and 2035–2064 at Lacrosse, WA and 300 kg ha^{-1} for conventional tillage during 1970–1999 at Moro, OR. Although not apparent in Fig. 6, the upper range in annual soil loss approached 307,000 and 259,000 kg ha^{-1} for conventional tillage during respectively 1970–1999 and 2035–2064 at Lacrosse, WA; 68,400 and 47,400 kg ha^{-1} for conservation tillage and 492,000 and 282,000 kg ha^{-1} for conventional tillage during respectively 1970–1999 and 2035–2064 at Lind, WA; and 21,700 kg ha^{-1} for conservation tillage during 1970–1999 at Moro, OR. The range in annual soil loss decreased from 1970–1999 to 2035–2064 for both tillage practices at each of the three locations.

Visual assessment of average soil loss across years in Fig. 6 suggests that soil loss is more variable during 1970–1999 than 2035–2064. Indeed, the SE of soil loss simulated by WEPS was greater for all locations, rotations, and soils during 1970–1999. The SE in soil loss across the 30 fallow years ranged from 33 kg ha^{-1} for conservation tillage at Lacrosse, WA to 4743 kg ha^{-1} for conventional tillage on Ritzville silt loam at Lind, WA during 1970–1999 and from 15 kg ha^{-1} for conservation tillage at Moro, OR to 1298 kg ha^{-1} for conventional tillage at Lacrosse, WA during 2035–2064. The SE in PM10 loss across the 30 fallow years was also greater during 1970–1999 than 2035–2064. The CV in soil loss simulated by WEPS across the 30 fallow years, however, was similar during 1970–1999 and 2035–2064. The CV in soil loss typically differed by < 10% between 1970–1999 and 2035–2064 for the same soil and tillage practice at a given location. A notable exception was conservation tillage at Lind, WA. The CV in soil loss for conservation tillage on Ritzville silt loam was 111% during 1970–1999 and 290% during 2035–2064 while the CV in soil loss for conservation tillage on Shano silt loam was 115% during 1970–1999 and 292% during 2035–2064. The small and inconsistent difference in the CV in soil loss between 1970–1999 and 2035–2064 suggest similarity in climate extremes which govern extreme wind erosion events. These extreme events would outweigh smaller wind erosion events for an ensemble of WEPS simulations performed using climate data from each of the 18 GCM's during 1970–1999 and 2035–2064.

4. Conclusions

Soil and PM10 loss associated with wind erosion was simulated by WEPS for a changing climate in the Columbia Plateau of the Pacific Northwest United States where windblown dust originating from agricultural lands contributes to poor air quality. Climate projections for an ensemble of 18 GCM's suggest that the climate will be wetter and warmer during 2035–2064 than 1970–1999. Based on current and future grain yield and climate at three locations, soil and PM10 losses will likely decrease by 25–84% during 2035–2064. The reduction in soil and PM10 losses may be due in part to higher grain yield and related biomass projected during 2035–2064. Soil and PM10 losses were greater from a WW-Cam-SF rotation than WW-SF rotation when conservation tillage practices are employed during the fallow phase of the rotations.

Despite accounting for differences in the length of each rotation, average annual soil and PM10 losses remain higher for the WW-Cam-SF rotation than the WW-SF rotation. Thus, stringent conservation practices may be required when introducing camelina into WW-SF rotations to reduce the risk of wind erosion in the region. Although the SE in annual soil and PM10 losses simulated by WEPS was greater during 1970–1999, the comparable CV in annual soil and PM10 losses suggest a similarity in climate extremes during 1970–1999 and 2035–2064.

The reduction in soil loss during 2035–2064 as compared to 1970–1999 is likely associated with changes in both climate and surface characteristics that influence wind erosion processes. While enhanced biomass production may offer greater protection to the soil from wind erosion, a reduction in wind speed could also decrease the potential for wind erosion during 2035–2064. This uncertainty and complexity of factors (e.g. climate, biology, and soil) that drive wind erosion requires further studies to identify the cause of the reduction in wind erosion during 2035–2064 as compared to the historical climate.

References

Abatzoglou, J., 2013. Development of gridded surface meteorological data for ecological applications and modelling. Int. J. Climatol. 33, 121–131.

Abatzoglou, J.T., Brown, T.J., 2012. A comparison of statistical downscaling methods suited for wildfire applications. Int. J. Climatol. 32, 772–780.

Ashkenazy, Y., Yizhaq, H., Tsoar, H., 2011. Sand mobility under climate change in the Kalahari and Australian deserts. Clim. Change 112, 901–923.

Bilbro, J.D., Fryrear, D.W., 1994. Wind erosion losses as related to plant silhouette and soil cover. Agron. J. 86, 550–553.

Böhner, J., Gross, J., Riksen, M., 2004. Impact of land use and climate change on wind erosion: prediction of wind erosion activity for various land use and climate scenarios using the WEELS wind erosion model. In: Goossens, D., Riksen, M. (Eds.), Wind Erosion and Dust Dynamics: Observations, Simulations, Modelling. ESW Publications, Wageningen, The Netherlands.

Buschiazzo, D.E., Zobeck, T.M., 2008. Validation of WEQ, RWEQ, and WEPS wind erosion for different arable land management systems in the Argentinean Pampas. Earth Surf. Process. Landf. 33, 1839–1850.

Chen, L., Zhao, H., Han, B., Bai, Z., 2014. Combined use of WEPS and Models-3/CMAQ for simulating wind erosion source emission and its environmental impact. Sci. Total Environ. 466–467, 762–769.

Coen, G.M., Tatarko, J., Martin, T.C., Cannon, K.R., Goddard, T.W., Sweetland, N.J., 2004. A method for using WEPS to map wind erosion risk of Alberta soils. Environ. Model. Softw. 19, 185–189.

European Environment Agency, 2012. Climate Change, Impacts and Vulnerability in Europe 2012: An indicator-based Report. Report no. 12, Copenhagen, Denmark.

Feng, G., Sharratt, B., 2007. Validation of WEPS for soil and PM10 loss from agricultural fields within the Columbia Plateau of the United States. Earth Surf. Process. Landf. 32, 743–753.

Fryrear, D.W., 1985. Soil cover and wind erosion. Trans. Am. Soc. Agric. Eng. 28, 781–784.

Funk, R., Skidmore, E.L., Hagen, L.J., 2004. Comparison of wind erosion measurements in Germany with simulated soil losses by WEPS. Environ. Model. Softw. 19, 177–183.

Gao, Q., Ci, L., Yu, M., 2002. Modeling wind and water erosion in northern China under climate and land use changes. J. Soil Water Conserv. 57, 46–55.

Goyette, S., Brasseur, O., Beniston, M., 2003. Application of a new wind gust parameterization: multiscale case studies performed with the Canadian regional climate model. J. Geophys. Res., 108. http://dx.doi.org/10.1029/2002JD002646.

Hagen, L., 1991. A wind erosion prediction system to meet user needs. J. Soil Water Conserv. 46, 106–111.

Hagen, L.J., 1996. Crop residue effects on aerodynamic processes and wind erosion. Theor. Appl. Climatol. 54, 39–46.

Hagen, L.J., 2004. Evaluation of the Wind Erosion Prediction System (WEPS) erosion submodel on cropland fields. Environ. Model. Softw. 19, 171–176.

Hagen, L., Woodruff, N.P., 1973. Air pollution from dust storms in the Great Plains. Atmos. Environ. 7, 323–332.

IPCC, 2007. Climate change, 2007: impacts, adaptation and vulnerability. In: Parry, M., Canziani, O., Palutikof, J., Vnerinden, P., Hanson, C. (Eds.), Contribution of Working Group II to the Fourth Assessment Report of the Intergovernmental Panel on Climate Change. Cambridge University Press, Cambridge, United Kingdom, p. 976.

IPCC. 2013. Climate change, 2013. The physical science basis. In: Stocker, T.F., Qin, D., Plattner, G.-K., Tignor, M., Allen, S.K., Boschung, J., Nauels, A., Xia, Y., Bex, V., Midgley, P.M. (Eds.), Contribution of Working Group I to the Fifth Assessment Report of the Intergovernmental Panel on Climate Change. Cambridge University Press, Cambridge, United Kingdom, p. 1535.

Lee, J.L., Phillips, D.L., Dodson, R.F., 1996. Sensitivity of the US Corn Belt to climate change and elevated CO2: II. Soil erosion and organic carbon. Agric. Syst. 52, 503–521.

Lee, J.J., Phillips, D.L., Benson, V.W., 1999. Soil erosion and climate change: assessing potential impacts and adaptation practices. J. Soil Water Conserv. 54, 529–536.

Lemmen, D.S., Vance, R.E., Wolfe, S.A., Last, W.M., 1997. Impacts of future climate change on the southern Canadian Prairies: a paleoenvironmental perspective. Geosci. Canada 24, 121–133.

Liddicoat, C., Hayman, P., Alexander, B., Rowland, J., Maschmedt, D., Young, M.-A., Hall, J., Herrmann, T., Sweeney, S., 2012. Climate change, wheat production and erosion risk in South Australia's cropping zone: linking crop simulation modelling to soil landscape mapping. Government of South Australia, Department of Environment, Water and Natural Resources.

Maurer, T., Gerke, H.H., 2011. Modelling Aeolian sediment transport during initial soil development on an artificial catchment using WEPS and aerial images. Soil Tillage Res. 117, 148–162.

Mote, P., Brekke, L., Duffy, P.B., Maurer, E., 2011. Guidelines for constructing climate scenarios. Eos, Trans. Am. Geophys. Union 92, 257–258.

Munson, S.M., Belnap, J., Okin, G., 2011. Responses of wind erosion to climate-induced vegetation changes on the Colorado Plateau. Proc. Natl. Acad. Sci. 108, 3854–3859.

Pryor, S.C., Schoof, J.T., Barthelmie, R.J., 2006. Winds of change?: projections of near-surface winds under climate change scenarios. Geophys. Res. Lett. 33. http://dx.doi.org/10.1029/2006GL026000.

Pryor, S.C., Barthelmie, R.J., Young, D.T., Takle, E.S., Arritt, R.W., Flory, D., Gutowski, W.J., Nunes, A., Roads, J., 2009. Wind speed trends over the contiguous United States. J. Geophys. Res. 114. http://dx.doi.org/10.1029/2008JD011416.

Rupp, D.E., Abatzoglou, J.T., Hegewisch, K.C., Mote, P.W., 2013. Evaluation of CMIP5 20th century climate simulations for the Pacific Northwest USA. J. Geophys. Res. 118, 10884–10906. http://dx.doi.org/10.1002/jgrd.50843.

Schillinger, W.F., Young, D.L., 2004. Cropping systems research in the world's driest rainfed wheat region. Agron. J. 96, 1182–1187.

Schillinger, W.F., Papendick, R.I., Guy, S.O., Rasmussen, P.E., Van Kessel, C., 2006. Dryland cropping in the western United States. In: Peterson, G.A., Unger, P.W., Payne, W.A. (Eds.), Dryland Agriculture. Agronomy Monograph 23. American Society of Agronomy, Madison, WI, pp. 365–393.

Schillinger, W.F., Wysocki, D.J., Chastain, T.G., Guy, S.O., Karow, R.S., 2012. Camelina: plaing date and method effects on stand establishment and seed yield. Field Crops Res. 130, 138–144.

Sharratt, B., Lauer, D., 2006. Particulate matter concentration and air quality affected by windblown dust in the Columbia Plateau. J. Environ. Qual. 35, 2011–2016.

Sharratt, B.S., Wendling, L., Feng, G., 2012. Surface characteristics of a windblown soil altered by tillage intensity during summer fallow. Aeol. Res. 5, 1–7.

Sharratt, B.S., Vaddella, V.K., Feng, G., 2013. Threshold friction velocity influenced by wetness of soils within the Columbia Plateau. Aeol. Res. 9, 175–182.

Sharratt, B., Schillinger, W.F., 2014. Windblown dust potential from oilseed cropping systems in the Pacific Northwest United States. Agron. J. 106, 1–6.

Stöckle, C.O., Nelson, R.L., Higgins, S., Brunner, J., Grove, G., Boydston, R., Whiting, M., Kruger, C., 2009. Assessment of climate change impact on eastern Washington agriculture. In: Elsner, M., Littell, J., Binder, L. (Eds.), The Washington Climate Change Impacts Assessment. Center for Science in the Earth System, University of Washington, Seattle, WA.

Taylor, K.E., Stouffer, R.J., Meehl, G.A., 2012. An overview of CMIP5 and the experiment design. Bull. Am. Meteorol. Soc. 93, 485–498.

Thomson, A.M., Brown, R.A., Ghan, S.J., Izaurralde, R.C., Rosenberg, N.J., Leung, L.R., 2002. Elevation dependence of winter wheat production in eastern Washington state with climate change: a methodological study. Clim. Change 54, 141–164.

van Donk, S.J., Wagner, L.E., Skidmore, E.L., Tatarko, J., 2005. Comparison of the Weibull Model with measured wind speed distributions for stochastic wind generation. Trans. Am. Soc. Agric. Eng. 48, 503–510.

World Glacier Monitoring Service, 2008. Global Glacier Changes: Facts and Figures. World Glacier Monitoring Service, University of Zurich, Switzerland.

Wysocki, D.J., Chastain, T.G., Schillinger, W.F., Guy, S.O., Karow, R.S., 2013. Camelina: seed yield response to applied nitrogen and sulfur. Field Crops Res. 145, 60–66.